Received <day> <Month>, <year>; | Revised <day> <Month>, <year>; | Accepted <day> <Month>, <year>

DOI: xxx/xxxx

ARTICLE TYPE

Bayesian Hierarchical Model for Immune Responses to Leishmania - a tick borne Co-Infection Study

Felix M. Pabon-Rodriguez*[1] | Grant D. Brown[1] | Breanna M. Scorza[2,3] | Christine A. Petersen[2,3]

[1]Department of Biostatistics, The University of Iowa College of Public Health, Iowa City, Iowa, United States
[2]Department of Epidemiology, The University of Iowa College of Public Health, Iowa City, Iowa, United States
[3]Center for Emerging Infectious Diseases, The University of Iowa College of Public Health, Iowa City, Iowa, United States

Correspondence
*Felix M. Pabon-Rodriguez
Email: felix-pabon-rodriguez@uiowa.edu

Present Address
Department of Biostatistics, The University of Iowa College of Public Health, Iowa City, Iowa, United States

Abstract

While many Bayesian state-space models for infectious disease processes focus on population infection dynamics (e.g., compartmental models), in this work we examine the evolution of infection processes and the complexities of the immune responses within the host using these techniques. We present a joint Bayesian state-space model to better understand how the immune system contributes to the control of *Leishmania infantum* infections over the disease course. We use longitudinal molecular diagnostic and clinical data of a cohort of dogs to describe population progression rates and present evidence for important drivers of clinical disease. Among these results, we find evidence for the importance of co-infection in disease progression. We also show that as dogs progress through the infection, parasite load is influenced by their age, ectoparasiticide treatment status, and serology. Furthermore, we present evidence that pathogen load information from an earlier point in time influences its future value, and that the size of this effect varies depending on the clinical stage of the dog. In addition to characterizing the processes driving disease progression, we predict individual and aggregate patterns of Canine Leishmaniasis progression. Both our findings and the application to individual-level forecasting are of direct clinical relevance, presenting possible opportunities for application in veterinary practice and motivating lines of additional investigation to better understand and predict disease progression. Finally, as an important zoonotic human pathogen, these results may support future efforts to prevent and treat human Leishmaniosis.

KEYWORDS:
Bayesian modeling, Co-infection, Immune Responses, Canine Leishamiasis, Longitudinal

1 | AUTHOR SUMMARY

The immune system is a complex network which involves organs, cells, and proteins working together with the main purpose of protecting the body against harmful microorganisms such as bacteria, viruses, fungi, and toxins. To explore and study the responses of the host immune system during the course of a disease, we modeled the interaction between pathogen load, antibody responses, and the clinical presentation of this complex system. Specifically, we focused on *Canine Leishmaniasis* (CanL), a vector-borne disease caused by a parasite, which affects internal organs of the body and is known to be fatal if patients remain untreated. In addition, we also considered the impact of possible co-infections with other diseases, which could potentially interact with many disease processes and contribute to different outcomes for infected subjects. With CanL specifically, we

consider the presence of *Borrelia*, *Anaplasma*, *Ehrlichia,* and Heartworm. In general, one limitation in vaccination strategies is a focus on neutralizing antibodies, without incorporating broader complexities of immune responses. Here, we explore this complexity by jointly considering the interaction between pathogen and antibody development with the purpose of improving our understanding of the processes of disease progression and natural immunity.

In this paper, we present a Bayesian Hierarchical Model (BHM) specification for immune responses to a Leishmania-tick borne co-infection study. This model implementation is based on the general vector autoregressive (VAR) model, adapted to the problem under study. We present evidence that pathogen load pathogen load information from an earlier point in time influences its future value, and that the size of this effect varies depending on the CanL clinical stage of the dog. In addition to characterizing evidence for the processes driving disease progression, we predict individual and aggregate patterns of CanL progression.

The structure of this paper starts in Section 2 with an introduction to CanL infection as well as a discussion of possible co-infection with other pathogens. In Section 3, we include a description of the motivating prospective study along with the measured individual level variables, a definition of the clinical signs of leishmaniosis infection, and a description of the available data coming from the study. In addition, this section explains the dynamic process and corresponding model specification, via Bayesian methodology. A summary of prior distributions for model parameters, model implementation details, and convergence diagnostics are also included. In Section 4, we provide summary results from the posterior distribution as well as a summary of the corresponding disease progression forecasts. In Section 5, we discuss the results and describe future considerations to improve and extend the model.

2 | INTRODUCTION: CANINE LEISHMANIASIS

Visceral Leishmaniasis (VL) is a life-threatening parasitic disease endemic in 98 countries, with an estimated 50,000 - 90,000 new cases annually according to the World Health Organization (WHO). Despite this widespread distribution, VL is considered a neglected tropical disease. There is no approved human vaccine, and current treatments can have adverse side effects and do not lead to clinical cure. This can lead to recrudescence of disease[1]. VL is caused by family of parasites in the *Leishmania (L.) donovani* complex, including *L. infantum*. It is known that *L. infantum* is a zoonotic infectious disease with dogs as the predominant reservoir. Spatial modeling has shown human VL incidence positively associates with prevalence of *L. infantum* infection among dogs in an endemic area[2]. Therefore, limiting transmission among and from infected dogs is an important target for preventing human infections. However, our understanding of CanL transmission dynamics is hampered by a lack of ability to accurately predict clinical CanL progression within the canine reservoir.

In addition to helping understand *L. infantum* transmission, elucidating CanL clinical progression dynamics can give us important pathophysiological insight into human VL, as the canine immune response to *L. infantum* closely mirrors human disease[3]. In both humans and dogs, the majority of *L. infantum* infections are sub-clinical, controlled by a Type 1 immune response. However, dogs can still be infectious to the insect vector during this time[4,5]. For reasons that are not well defined, clinical progression occurs in a subset of dogs and people, where Type 1 immunity wanes and parasite load increases. Such progression leads to increased transmission potential.

Diagnosis of CanL is based on a combination of molecular and clinical factors. Molecular diagnostics include serology, which may indicate current infection or previous exposure, and Polymerase chain reaction (PCR) of *Leishmania* deoxyribonucleic acid (DNA) from whole blood, which indicates current infection above the threshold of detection. Increasing parasitemia level is associated with disease progression[6]. Anti-*Leishmania* antibodies produced during infection are generally non-protective, and increasing serological titers are also associated with worsening disease status[7]. As infected dogs progress to early CanL, clinical signs of disease are non-specific (i.e. weight loss, lymphadenopathy, lethargy) and molecular diagnostics may or may not be positive. As disease progresses, anemia and hypergammaglobulinemia usually precede chronic kidney disease and ultimately kidney failure if untreated[7].

In this work, we prospectively followed a cohort of dogs with sub-clinical *L. infantum* infection and collected longitudinal molecular diagnostic and clinical data to evaluate disease progression over 18 months. We used this data to develop a joint Bayesian state-space model to predict progression kinetics based on continuous diagnostic data and discrete clinical stages. We explore population progression rates, and present evidence for important dependencies among measured components of disease status. In particular, we find further evidence for the importance of co-infection status in CanL progression. Furthermore, we show that as dogs advance through the infection, their age, ectoparasiticide treatment indicator, and serology all impact parasite load. We also show that pathogen load information from a previous time influences its future value, and that the magnitude of

this effect varies depending on the dog's clinical state, where the effects of these clinical drivers are being measured via the model parameters. We also look into the model's suitability as a tool for predicting clinical disease progression.

One of the primary non-time-varying predictors of interest within the study is the output of the IDEXX 4Dx Plus SNAP test, which is a combined in vitro test for the detection of antigen to *Dirofilaria immitis*, antibodies to *Borrelia burgdorferi*, *Anaplasma phagocytophilum*, *Anaplasma platys*, *Ehrlichia canis*, and *Ehrlichia ewingii* in canine serum, plasma, or anticoagulated whole blood. It is known that previous or simultaneous infections of a host by multiple pathogen species (*spp.*) can complicate CanL clinical outcomes[8]. Some studies have shown that the presence of additional interacting pathogens can modify the immune response of affected host[9]. This phenomena of co-infection is of great importance in the progression of CanL[10]. By studying the effect of this predictor, we aim to measure the strength of its effect during the course of infection and identify different possible clinical outcomes for co-infected subjects. Within our CanL cohort, we specifically considered the effects of *Borrelia burgdorferi*, *Anaplasma spp.*, *Ehrlichia spp.*, and Heartworm exposure.

3 | MATERIALS AND METHODS

3.1 | Cohort Selection and Diagnostics

A prospective study was performed using a cohort of naturally *L. infantum* exposed, client-owned hunting dogs from the United States. Dogs were screened for CanL clinical signs by board certified veterinarians, tick-borne bacteria serology by IDEXX 4Dx Plus SNAP test, and *Leishmania* diagnostics: Real Time quantitative PCR (RT-qPCR) of whole blood and Dual Path Platform ® (DPP) Canine Visceral Leishmaniasis serological test[11,12]. The inclusion criteria is IDEXX 4Dx Plus SNAP test seronegative and positive on one *Leishmania* diagnostic test or having a *Leishmania* diagnostic positive dam or full sibling. On the other hand, exclusion criteria is more than 2 clinical signs of CanL or DPP reader value greater than 200 or IDEXX 4Dx Plus SNAP test seropositive. A total of fifty dogs were enrolled in the study and followed over the course of 18 months. The cohort was equally randomized into a tick prevention ectoparasiticide treatment or placebo group under a double-blind setting, and where the age range of dogs was from 0 to 11 years old.

3.2 | Variables

During the data collection period, diagnostic variables and clinical disease were assessed at three month intervals. This included RT-qPCR for parasite quantification in the blood of subjects. Pathogen load is then presented as the number of parasite equivalents per mL of blood, calculated from a standard curve of canine blood spiked with a known number of *L. infantum* promastigotes[11]. Relative quantification of anti-*Leishmania* antibody levels in subject sera was performed using an indirect Enzyme linked immunoassay (ELISA) against soluble *Leishmania* antigen (SLA). Wells of ELISA plates were coated with 200 ng/mL SLA obtained by repeated freeze-thaw of *L. infantum* promastigotes and probed with canine serum samples diluted 1:500. The optical density (OD) measured at 450 nm on a plate reader is shown as a ratio to a cut-off OD (average of control sample ODs + 3 standard deviations). OD ratios >1 indicate positive serology. Complete blood count and serum chemistry panels were performed by IDEXX Reference Labs.

The SNAP variable presents dichotomous results from the IDEXX 4Dx Plus SNAP test, which tests for serologic reactivity to tick-borne bacterial antigen from *Borrelia burgdorferi*, *Anaplasma spp.* , and *Ehrlichia spp.*, indicating previous exposure to these pathogens. Although all dogs were negative by 4Dx Plus SNAP test at enrollment, we observed that 44% of the dogs tested positive on the 4Dx Plus SNAP test at some point during the study period, which indicates co-infection between *L. infantum* and a tick-borne pathogen occurred during the study period. In addition, we considered results from the DPP serological test, which detects anti-*Leishmania* antibodies. DPP is similar to SLA ELISA, but more specific as it detects antibodies specific for recombinant chimeric k28 protein and results measured with a digital intensity reader. The mean and standard deviation in DPP results are 25.20 and 41.56, respectively. However, the DPP test was only performed at enrollment, while the SLA ELISA was performed at three month intervals. Finally, treatment with the ectoparasiticide medication sarolaner (Zoetis Inc.) or placebo was included. We have that 50% ($n = 25$) of the cohort was randomly assigned to each treatment group at enrollment.

3.3 | Model Specification

The clinical signs of *Leishmania* infection are known to vary widely as a consequence of several pathogenic mechanisms. Depending on the subject, different organs can be affected, and there is a diverse range of immune responses built by individual hosts. This variability and non-specificity of clinical manifestations makes diagnosis and treatment challenging. The diagnosis of CanL is performed based on clinicopathological manifestations and by confirmation of infection by using mainly serological and additional molecular techniques. In response to these challenges, Solano-Gallego et al.[7] proposed a system, identified as LeishVet score, that uses serological results, clinical signs, and laboratory findings to differentiate and categorize patients with CanL into stages. Stage 1 is used for a case of mild disease, Stage 2 for moderate disease, Stage 3 for severe disease, and Stage 4 to identify very severe, end stage disease. LeishVet is a group that proposed guidelines and recommendations designed primarily to help the veterinary clinician in the management of canine leishmaniosis. This LeishVet score system is helpful because it assists clinicians and veterinarians in determining the appropriate therapy, to predict prognosis, and implementing adequate follow-up steps required to help patients with CanL. In this study, physical exam findings, complete blood count, and serum chemistry values were used to stage CanL severity based on the LeishVet staging guidelines proposed by Solano-Gallego et al.[7]. We have modified the staging system slightly to include a Stage 0 representing no signs of disease.

When it comes to CanL studies, determining course of treatments is not an easy task, particularly when many unknown relationships between *Leishmania* infection and the immune system still remain unanswered. While various laboratory techniques are beneficial for answering questions pertaining a particular disease, it is always critical to have in mind that qPCR data should not be separated from data collected from other sources, such as clinicopathological and serological examinations[7,13], for determining clinical decision. Thus, rather than focusing on infectious agent transmission between individuals, the Bayesian model presented in this work is thought to be dynamic and interactive within the host.

To assess CanL disease progression of subjects over time, we took into account the LeishVet stages, pathogen load, and level of anti-*Leishmania* antibodies as explained in the previous section. Each dog was classified based on the scoring proposed by Solano-Gallego et al.[7]. We further aggregate this scoring into the qualitative categories described in Equation 1, for the ith dog at time $t+1$, where we defined disease status $D_{i,t+1}$ for the corresponding indexes. This categorization was encoded as separate indicator variables for each stage over time for each dog.

$$D_{i,t+1} = \begin{cases} 1\,(\text{Healthy}), & \text{if } LeishVet = 0 \text{ or } 1 \\ 2\,(\text{Asymptomatic}), & \text{if } LeishVet = 2 \\ 3\,(\text{Symptomatic}), & \text{if } LeishVet = 3 \text{ or } 4 \\ 4\,(\text{Removed}), & \text{if removed due to severe} \\ & \text{case of Leishmaniasis,} \end{cases} \tag{1}$$

Once an individual is infected with the parasite *L. infantum*, a replication process takes place. At the same time, the host immune mounts a response against the parasite. Therefore, parasitemia may fluctuate as these opposing processes occur, but systematic variation over time may indicate future trajectory of disease. One way to measure the pathogen status component of the overall dynamic process is through pathogen burden. For *Leishmania*, let us define $P_{i,t+1}$ to denote the pathogen load for the ith dog at time $t+1$, measured as the number of parasites per mL of blood. Further, let $A_{i,t+1}$ denote the anti-*Leishmania* antibody level measured by ELISA SLA OD ratio for the same indexes. As indicated in the previous section, disease status was assessed by the proposed variable $D_{i,t+1}$ as defined in Equation 1.

In Figure 1, we illustrate the model's temporal dependence structure with time index t and subject index i, which is constructed sequentially and dynamically. This diagram shows how each model component can either directly or indirectly influence each proximal state component. To capture the evolution of state over time, we assume that the future state for each model component is dependent on the full current state of the host (pathogen load, antibody levels, and disease state progression) via some functions, denoted by f_D, f_A, and f_P, describing the expected state at the next time point for each of the three main model components. In addition, the case history or any other fixed effects for the host was also considered to affect future state, which are encoded by X_i, a subject-specific row-vector containing non-time-varying predictors of progression characteristics. This structure could be considered a generalized vector-autoregressive model, though it has been tailored to the expected dependence structure of CanL progression. In general, we have a function f_D describing the disease progression in terms of clinical signs as depending on current immunopathogenic state, while the functions f_A and f_P describe the antibody levels and pathogen load

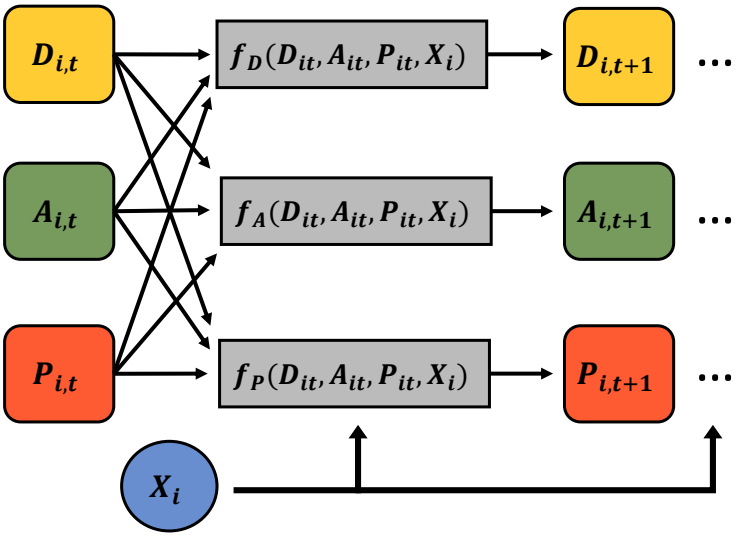

FIGURE 1 Dynamic Process. Graphical display of how the disease state (D), immune responses (A), and pathogen load (P) components are related to predict the future value of each state.

also as functions of previous or current state. In addition, these components can incorporate individual specific error components, capturing measurement error and individual level heterogeneity, which could be caused by clinical differences associated with the disease. Then, in general, the future state of these components are determined by these update functions, random errors, and parameters associated with the dynamic system, all of this under some distributional assumptions, as shown in Equation 3.

The precise specification of the update functions shown in Figure 1 could be as simple as linear functions of the three state components, in which case the model would reduce exactly to a VAR process. In addition, expansions could be considered (e.g., interactions, non-linear terms, basis expansions, or non-linear link functions coupled to the distribution of subsequent components). We propose to use a simple formulation with Gaussian distributions for pathogen load and antibody response, and a multinomial-logit link for disease status, where functional forms f_D, f_A and f_P are defined as shown in Equation 2.

$$
\begin{aligned}
f_D(D_{i,t}, P_{i,t}, A_{i,t}, X_i) &= \left[\pi_{i,t}^{(1)}, \pi_{i,t}^{(2)}, \pi_{i,t}^{(3)}, \pi_{i,t}^{(4)}\right] \\
\pi_{i,t}^{(k)} &= \frac{exp\left[M_{i,t}^{D(k)}\boldsymbol{\beta}_D^{(k)} + X_i\boldsymbol{\alpha}_D\right]}{1 + \sum_{g=1,2,3} exp\left[M_{i,t}^{D(g)}\boldsymbol{\beta}_D^{(g)} + X_i\boldsymbol{\alpha}_D\right]} \\
\pi_{i,t}^{(4)} &= 1 - \pi_{i,t}^{(1)} - \pi_{i,t}^{(2)} - \pi_{i,t}^{(3)} \\
f_A(D_{i,t}, P_{i,t}, A_{i,t}, X_i) &= M_{i,t}^{A}\boldsymbol{\beta}_A + X_i\boldsymbol{\alpha}_A \\
f_P(D_{i,t}, P_{i,t}, A_{i,t}, X_i) &= M_{i,t}^{P}\boldsymbol{\beta}_P + X_i\boldsymbol{\alpha}_P
\end{aligned}
\tag{2}
$$

For $N = 50$ dogs, and $T = 7$ time points, we have then a conditional layout on dependence structures, where each model component is distributed independently according to Equation 3. In the multinomial distribution, $\pi_{i,t}^{(k)}$ defines the probability that the ith dog at time t is classified with disease status k. The primary components of the model, which are denoted as P, A, and D, have design row vectors that change over study-time, denoted by $M_{i,t}^{P}$, $M_{i,t}^{A}$, and $M_{i,t}^{D}$, respectively. Non-time-varying predictors are captured in a subject-specific row vector X_i (intercept, age, SNAP, DPP, and an indicator for treatment).

For the evolution of pathogen load, $M_{i,t}^{P}$ captures current pathogen load, an interaction between disease stage and pathogen load, an interaction between disease stage and prior changes in pathogen load, and an interaction between disease stage and prior changes in antibody levels. On the other hand, the antibodies are modeled as dependent on current pathogen load and antibody levels as well as in the previously indicated interaction terms. In order to interpret whether a host response to an infection seems appropriate at a particular time point, it needs to be assessed in relation to the pathogen load that triggered the response. By using

current value of pathogen load and its interaction with disease stage, we are able to understand one of the most fundamental questions, which is the relationship between pathogen load and the severity of the disease. We explore this relationship in more detail by including interaction terms and prior information.

The main difference between the two row vectors $M_{i,t}^P$ and $M_{i,t}^A$ is the assumption that the production of antibodies depends on the production of pathogen load and current value of antibodies, but the pathogen load is not directly dependent on antibodies, which are generally non-neutralizing. For the qualitative disease stage, $M_{i,t}^D$ considers current disease stage and the interaction of the disease stage with current pathogen load, and interaction of the disease stage with current antibody levels. For this model specification, notice that the update functions from Figure 1 are defined to be the mean structures of the distribution.

The dimensions of the different subject-specific row vectors, denoted by $M_{i,t}$, vary by model components. For example, $M_{i,t}^P$ is a 1×10 matrix (or row vector), while $M_{i,t}^A$ and $M_{i,t}^D$ are a 1×8 and 1×3 row vectors, respectively. Each entry within these row vectors are scalars, representing different possible drivers of the model dependence. In the case of the subject-specific row vector X_i, which includes non-time-varying predictors and an intercept, its dimension is 1×5, which includes age group, dichotomous results from SNAP test, DPP results, and an indicator for treatment group. The elements in X_i are also scalars.

$$\begin{aligned} D_{i,t+1} &\sim \text{Multinomial}\big(1; f_D(D_{i,t}, P_{i,t}, A_{i,t}, X_i)\big) \\ A_{i,t+1} &\sim \mathcal{N}\big(f_A(D_{i,t}, P_{i,t}, A_{i,t}, X_i),\ \sigma_A^2\big) \\ P_{i,t+1} &\sim \mathcal{N}\big(f_P(D_{i,t}, P_{i,t}, A_{i,t}, X_i),\ \sigma_P^2\big) \end{aligned} \tag{3}$$

As disease progression for Leishmaniasis depends on both pathogen and immunological behavior[7,14], we included in the row vectors, both components as well as interaction terms with the disease status. To measure the strength of the effects of changing pathogen burden and antibody levels, we computed lag-1 differences for these quantities ($d_{i,t}^P$ and $d_{i,t}^A$). The row vectors also include the interaction of these lag-1 differences with clinical stage. Shang et al. showed[15] that age and external clinical status of dogs are associated with prevalence of *Leishmania* infection. In their study, dogs that were +1 year old had higher prevalence of *L. infantum* infection than younger dogs ($\leq$ 1 year old), resulting from most likely longer exposure to infective sand fly bites. We therefore included age group and clinical information (e.g. SNAP and DPP results at baseline, treatment group) in our row vector X_i. Notice that X_i is included in the three distributions in Equation 3. Finally, as shown by the second to last equation, the components of the row vector $M_{i,t}^D$ will contribute to the probability that a dog will be classified into a particular disease status. This term is important for measuring the transitions between the four different qualitative categories as described in Equation 1. Overall, this specification is a special case of the well studied VAR model, which has been applied in fields as diverse as immunology and econometrics[16,17,18]. In this case, we augment the model with a latent component for disease stage, and carefully constrain the temporal dependence structure to encode structural information about the problem, such as the varying effects of shifting antibody levels by disease stage.

Using the model definition as described by Equations 2 and 3, the joint likelihood can be defined by the product of the each probability density (or probability mass) function corresponding to each model components. In this case, we have two continuous outcomes (pathogen load and antibody levels) and one categorical (disease status). To facilitate the definition of the likelihood presented in Equation 4, let us define $\boldsymbol{\theta}_P = (\boldsymbol{\beta}_P, \boldsymbol{\alpha}_P, \sigma_P^2)'$ as the set of vectors associated with pathogen load. Similarly, we can define the set of parameters associated with the antibody levels and disease status as $\boldsymbol{\theta}_A = (\boldsymbol{\beta}_A, \boldsymbol{\alpha}_A, \sigma_A^2)'$ and $\boldsymbol{\theta}_D = (\boldsymbol{\beta}_D^{(1)}, \boldsymbol{\beta}_D^{(2)}, \boldsymbol{\beta}_D^{(3)}\boldsymbol{\alpha}_D)'$, respectively.

$$\begin{aligned} \mathcal{L}(\theta_P, \theta_A, \theta_D | P, A, D) &= \prod_{i=1}^{N}\left[f(P_{i,1})\cdot f(A_{i,1})\cdot f(D_{i,1})\cdot\prod_{t=2}^{T}\left\{f(P_{i,t}|P_{i,t-1},\theta_P)\cdot f(A_{i,t}|A_{i,t-1},\theta_A)\cdot f(D_{i,t}|D_{i,t-1},\theta_D)\right\}\right] \\ &\propto \prod_{i=1}^{N}\left[f(P_{i,1})\cdot f(A_{i,1})\cdot f(D_{i,1})\prod_{t=2}^{T}\left\{\left(\frac{1}{\sigma_P}exp\left\{-\frac{1}{2\sigma_P^2}(P_{i,t}-\eta_{i,t-1}^P)^2\right\}\right)\right.\right. \\ &\quad \left.\left.\cdot\left(\frac{1}{\sigma_A}exp\left\{-\frac{1}{2\sigma_A^2}(A_{i,t}-\eta_{i,t-1}^A)^2\right\}\right)\cdot\left(\pi_{i,t-1}^{(1)\ D_{i,t-1}^{(1)}}\cdot\pi_{i,t-1}^{(2)\ D_{i,t-1}^{(2)}}\cdot\pi_{i,t-1}^{(3)\ D_{i,t-1}^{(3)}}\cdot\pi_{i,t-1}^{(4)\ 1-\sum_{g=1}^{3}D_{i,t-1}^{(g)}}\right)\right\}\right] \end{aligned} \tag{4}$$

Here we have that the mean expressions for each normal density distribution are defined as $\eta_{i,t-1}^P = M_{i,t}^P\boldsymbol{\beta}_P + X_i\boldsymbol{\alpha}_P$, and $\eta_{i,t-1}^A = M_{i,t}^A\boldsymbol{\beta}_A + X_i\boldsymbol{\alpha}_A$, respectively. The expressions for the $\pi_{i,t-1}^{(k)}$ are presented in the last two formulas of Equation 3, while $D_{i,t-1}^{(k)}$ for $k = 1, 2, 3$ are defined as indicators, where equals 1 if $D_{i,t-1}^{(k)} = k$ and 0 otherwise, which are defined based in Equation 1. Note that a proportionality notation is used being in the second line of the likelihood, which helps on factoring out all of

the constants or fixed quantities. In addition, notice that we defined our baseline category in the multinomial distribution as $D^{(4)}_{i,t-1} = 1 - \sum_{g=1}^{3} D^{(g)}_{i,t-1}$.

3.4 | Disease Progression Forecasting

Although the structure of a posterior predictive distribution can sometimes be calculated analytically, simulations are frequently used to obtain such forecasts. In this work, disease progression forecasts were obtained using a sampling process (simulations) from the posterior distributions, following these steps:

(i) Sample a value from the posterior distributions of each parameter,

(ii) Obtain the estimated model components (predicted outcomes) from the Bayesian model specification in Equation 3, and

(iii) Repeat steps (i) and (ii) for $S = 1000$ times ($s = 1, 2, 3 \ldots, S$), where S represent the number of simulations performed.

3.5 | Computation and Model Diagnostics

To fit the Bayesian hierarchical model presented in this work, we coded and implemented a Metropolis-Hastings within Gibbs algorithm in R [19,20], to obtain posterior samples of model parameters and latent quantities. A general description of this Markov Chain Monte Carlo (MCMC) approach is provided by Liu [21] and Carlin [22].

We employed proper prior distributions to impose penalties for large regression weights in order to promote model stability and computational tractability. Standard independent normal prior distributions, $\mathcal{N}(0, 1)$, were used for the conditional and unconditional effects ($\boldsymbol{\beta}$'s) as well as for the parameters associated with non-time-varying predictors ($\boldsymbol{\alpha}$'s), in order to shrink these effects towards zero. A gamma prior distribution, $\Gamma(1, 1)$, was used for variance terms (σ^2's). Posterior results are based on a set of 3 chains of 25,000 iterations each.

To assess the convergence of the parameters, a Gelman-Rubin diagnostic was computed using the `coda` package in R [23]. The Gelman-Rubin criterion evaluates convergence by comparing within and between chain variability, which requires at least two MCMC chains to be calculated. As a rule to assess convergence, we used a value of 1.1 as a threshold. We say that a factor below 1.1 indicates that the parameter has reached convergence, which was achieved by all parameters in the model. The code implementing the sampler and associated full conditional distributions that were derived are linked in the supplemental material: https://github.com/fpabonrodriguez/Research-Project-BHM.

4 | RESULTS

The trajectories of observed pathogen loads and antibody levels over each of the seven time points, each separated by three months, are shown in Figure 2. The black line shows the mean trajectory of the subjects. This cohort enrolled dogs with asymptomatic CanL, therefore while most subject's parasitemia and antibody level trajectories illustrate a steady state or slow progression of the disease, we also observe several examples indicative of rapid changes to the immunopathogenic state, since the loss of immune control over pathogen replication is known to occur as disease progresses. This low production of antibodies agrees with previous findings in dogs with subclinical or early disease. Increasing antibody levels are seen in a subset of dogs, which has been shown to occur in dogs experiencing clinical progression.

The number of dogs classified into each disease stage over time is shown in Table 1. At the beginning of the study, most of the dogs were classified as either healthy or asymptomatic; the remaining two categories are symptomatic and removed. Due to unforeseen circumstances, the disease status for the second time point (month 6) was not able to be collected, and some other missing values were also reported in different time points for pathogen load and antibody levels due to random external events unrelated to the status of the dogs. Since these entries were not directly observed, they were considered as latent variables and imputed within the Bayesian analysis. The last two rows of the table indicates the number of unobserved entries at each time point, and the total number of subjects at each time point, which is 50, respectively.

In terms of the study's findings, we found moderate to strong evidence of temporal dependence across pathogen load, antibody levels, and illness status throughout CanL infection, meaning that previous behaviors of these components had a moderate to strong influence on their future values. To summarize these effects, explanations and interpretations of the results from this Bayesian analysis are presented, which pertains to Table 2. In general, this table shows a summary of the posterior results for

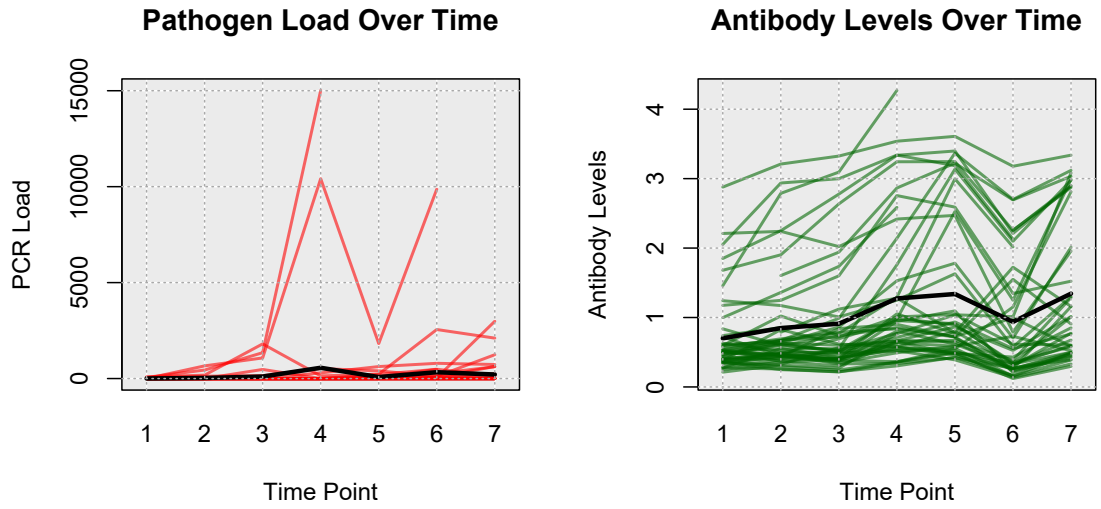

FIGURE 2 Pathogen Load and Antibody Level Kinetics. (Left plot) *Leishmania* pathogen load over time, expressed as the number of parasites per mL of blood. (Right plot) Anti-*Leishmania* antibody level over time expressed as the ratio to control cut-off. In both plots, the black line represents mean population trajectories. Each line represents a single dog's trajectory. Each time point corresponds to 3 elapsed months.

TABLE 1 Disease Status Counts. Observed number of dogs in each category of the disease state component of the Bayesian model.

	Time Point						
Disease Status	**1**	**2**	**3**	**4**	**5**	**6**	**7**
1 = Healthy	32	0	26	27	23	21	19
2 = Asymptomatic	16	0	21	18	22	19	19
3 = Symptomatic	2	0	0	1	0	4	2
4 = Removed	0	0	0	0	1	1	3
Missing (NA)	0	50	3	4	4	5	7
Total	50	50	50	50	50	50	50

all parameters in the model, including posterior means, standard deviation (SD), 95% credible intervals (Cr-I) and posterior probabilities for each parameter of being positive, which are being used for assessing the strength of evidence for corresponding parameters. The posterior probabilities of positive lag-1 dependence were 0.840 for pathogen load, and approximately 1 for antibody levels, and disease status 1 and 2, respectively. In contrast, the coefficient for disease status 3 was negative (posterior probability of negative lag-1 is 0.874). This last result could be due to the fact that dogs in clinical stage 3 (symptomatic) have presumably developed regulatory responses against the infection at a given time, leading to the production of important immunological cells such as CD4+ and CD8+ T cells, B cells, and macrophages[24,25,26], which can cause a reduction and control of pathogen production.

In addition, we found that pathogen load dependence on previous values varied by stage; the conditional interaction effect on pathogen load of lag-1 change in pathogen load for stage 2 dogs had a posterior mean of -0.874 with 95% Cr-I $[-1.110, -0.647]$ and posterior probability 0.999 that the true parameter is less than zero. This result tells us that subjects in the asymptomatic stage of the disease could show some decrease in the pathogen burden as time passes, which is consistent with the discussion from Petersen et al.[27], where it was shown that parasite load decreases once the inflammatory response from the immune system is active. We find moderate evidence that co-infection status (measured via 4Dx SNAP test) and dog age were associated with

increased parasite load overall (posterior probabilities of being positive are 0.740 and 0.828), as well as that the sarolaner treatment group had lower overall parasite loads (posterior probability of being negative of 0.860). Consistent with expectation, we also find compelling evidence that stronger DPP responses were associated with higher pathogen burden (posterior probability of being positive of 0.921).

In terms of antibodies, several compelling effects emerge. First, we find strong evidence that co-infection status (4Dx SNAP test) was associated with increased antibody levels, with a posterior probability of being positive of 0.981. This effect has a posterior mean of 0.014 with 95% Cr-I $[0.001, 0.027]$. This is an important result, since testing for serologic reactivity to tick-borne bacterial antigens can help us understand how the production of *Leishmania*-antibodies and the general inflammatory response could be affected by the presence of other pathogens [13]. In addition, stronger DPP responses were associated with higher antibody levels (posterior probability 0.975), which is expected since the DPP serological test also detects anti-*Leishmania* antibodies similar to SLA ELISA. We also found that the conditional interaction effect on antibody levels of lag-1 change in antibody levels for stage 1 dogs had a posterior mean of -0.392 with 95% Cr-I $[-0.591, -0.198]$ and posterior probability approximately 1 that the true parameter is less than zero.

In addition to characterizing evidence for the processes driving disease progression, we also investigated the degree to which the presented Bayesian model can predict individual and aggregate patterns of CanL progression. Using posterior predictive distributions based on parameters drawn from the converged MCMC samplers, we investigated different outcome patterns for dogs decreasing, not changing, and increasing clinical status over time. For this context, we identified $n^* = 4$ dogs within the same cohort based on four different outcomes scenarios, but assuming that only the information from the first two time points were available. The goal was to predict the pathogen load, antibody level and probabilities of the dogs to be classified in each disease status for additional points in time, and compare estimated trajectories from the observed trajectories.

For pathogen load and antibody level, we plot the predicted trajectories over time for each of the subjects, as well as the marginal probabilities of being in a particular disease state at each time point. We hypothesize that disease patterns can be predicted using diagnostic parameters with six months between measurements. This configuration has direct clinical relevance; veterinarian assessment of these or similar diagnostic variables for a given dog 6 months apart could be used to predict the future change in clinical status for that patient. Our model was constructed in such a way that allows us to use available data from the immediate past or present, and predict outcomes farther away in time. Since predictions in a 6 months interval were preferred, we can still use the information on a 3-month basis and make the predictions. Clearly, the amount of available data and the frequency of observed progression events will affect the predictive performance of the model.

Figures 3 and 4 show the predicted pathogen load and antibody level trajectories for the four subjects, based on different outcome patterns, respectively. For each prediction, we considered 80% and 95% prediction intervals, and a line representing the mean trajectories. In addition, we plotted the observed trajectories of the dogs. From this simple prediction setting, we were able to capture some of the observed trajectories of the dogs for the antibody levels. For pathogen load, the mean trajectory of the simulations was higher than the observed data for 3 out the 4 dogs, and close to the observed data for first dog.

In Figure 5, we present the posterior predicted marginal probabilities of the dogs being classified in a particular disease state over time. From these plots, we observe that the probabilities of a severe case of Leishmaniasis (disease status 4) increases from 0% to approximately 15% for all of these dogs, no matter their initial status. These four dogs started from a healthy or asymptomatic state. In addition, the probabilities of staying healthy reduced to approximately 38% for dogs 2 and 4, but it increases to around 35% for dogs 1 and 3. The presented model was able to capture several expected behaviors that were backed up by research. Dogs treated with sarolaner, for example, had lower total parasite burdens, and DPP serological test findings were linked to a higher pathogen burden. Our approach will benefit clinicians and veterinarians by allowing them to better understand immune responses and *Leishmania* infection control throughout time.

5 | DISCUSSION

There are several competing statistical and mathematical modelling approaches which could be applied to this problem, and to the best of our knowledge there is no single traditional approach which has universal acceptance in the proposed modelling setting. In the case of Frequentist methods, we felt that relying on asymptotic arguments for the short longitudinal follow-up would be sub-optimal. Moreover, we have a strong philosophical preference for Bayesian models, which are less likely to make strong and incorrect conclusions regarding hypotheses of interest due to the shrinkage effect of prior distributions [28], and have a strong axiomatic foundation [29]. When considering mathematical models, we felt that Bayesian methods are preferable

TABLE 2 Posterior Summary Results. Posterior summary of the three MCMC chains. In this summary, posterior means, standard deviation, and 95% credible intervals are provided, organized by outcome model (pathogen, antibodies and disease status). In addition, posterior probabilities of the parameters being positive are included in the last column. A brief description of these parameters are presented in the second column. The symbol * represents interaction of the indicated model elements.

Parameter	Interpretation	Mean	SD	95% Cr-I	Prob > 0
Pathogen Load (P)					
$\beta_{P,1}$	Pathogen Load	0.7049	0.7243	[-0.6768, 2.2512]	0.8433
$\beta_{P,2}$	Pathogen Load * (D=1)	0.1707	0.8839	[-1.5822, 1.8942]	0.5767
$\beta_{P,3}$	Pathogen Load * (D=2)	0.4538	0.7250	[-1.0940, 1.8612]	0.7506
$\beta_{P,4}$	Pathogen Load * (D=3)	-0.0323	0.9391	[-1.8752, 1.7981]	0.4868
$\beta_{P,5}$	(D=1) * Difference in Pathogen Load	0.1183	0.9555	[-1.7628, 2.0052]	0.5483
$\beta_{P,6}$	(D=2) * Difference in Pathogen Load	-0.8736	0.1237	[-1.1104, -0.6468]	0.0006
$\beta_{P,7}$	(D=3) * Difference in Pathogen Load	-0.0102	0.9767	[-1.9241, 1.8926]	0.4942
$\beta_{P,8}$	(D=1) * Difference in Antibody Levels	0.0163	0.0406	[-0.0587, 0.0925]	0.6698
$\beta_{P,9}$	(D=2) * Difference in Antibody Levels	-0.0030	0.0507	[-0.0822, 0.0754]	0.4644
$\beta_{P,10}$	(D=3) * Difference in Antibody Levels	0.0525	0.2307	[-0.3916, 0.5111]	0.5929
σ^2_P	Variance in Pathogen Load	0.0215	0.0058	[0.0194, 0.0231]	-
$\alpha_{P,1}$	Intercept	-0.0005	0.0095	[-0.0160, 0.0144]	0.4813
$\alpha_{P,2}$	Age group	0.0017	0.0056	[-0.0025, 0.0063]	0.8276
$\alpha_{P,3}$	SNAP results	0.0020	0.0044	[-0.0037, 0.0074]	0.7409
$\alpha_{P,4}$	DPP results	0.0103	0.0100	[-0.0041, 0.0250]	0.9211
$\alpha_{P,5}$	Treatment group	-0.0027	0.0050	[-0.0082, 0.0026]	0.1334
Antibodies Level (A)					
$\beta_{A,1}$	Pathogen Load	-0.1662	0.3397	[-0.7823, 0.4588]	0.2894
$\beta_{A,2}$	Antibody Levels	0.8976	0.0589	[0.7931, 1.0084]	0.9999
$\beta_{A,3}$	(D=1) * Difference in Pathogen Load	0.6141	0.9863	[-1.3045, 2.5770]	0.7330
$\beta_{A,4}$	(D=2) * Difference in Pathogen Load	0.4121	0.2532	[-0.0764, 0.8862]	0.9510
$\beta_{A,5}$	(D=3) * Difference in Pathogen Load	0.0888	0.9938	[-1.8698, 2.0246]	0.5364
$\beta_{A,6}$	(D=1) * Difference in Antibody Levels	-0.3924	0.1008	[-0.5912, -0.1977]	0.0003
$\beta_{A,7}$	(D=2) * Difference in Antibody Levels	-0.1200	0.1137	[-0.3297, 0.0877]	0.1280
$\beta_{A,8}$	(D=3) * Difference in Antibody Levels	-0.1632	0.4645	[-1.1384, 0.7042]	0.3730
σ^2_A	Variance in Antibody Levels	0.0515	0.0039	[0.0473, 0.0560]	-
$\alpha_{A,1}$	Intercept	-0.0079	0.0179	[-0.0433, 0.0279]	0.3129
$\alpha_{A,2}$	Age group	-0.0034	0.0079	[-0.0137, 0.0076]	0.2705
$\alpha_{A,3}$	SNAP results	0.0141	0.0067	[0.0009, 0.0267]	0.9811
$\alpha_{A,4}$	DPP results	0.0470	0.0229	[-0.0004, 0.0876]	0.9747
$\alpha_{A,5}$	Treatment group	0.0048	0.0077	[-0.0081, 0.0172]	0.7721
Disease Status (D)					
$\beta_{D1,1}$	(D=1)	1.8619	0.2182	[1.4430, 2.2855]	0.9999
$\beta_{D1,2}$	(D=1) * Pathogen Load	0.0064	0.9901	[-1.9069, 1.9523]	0.5044
$\beta_{D1,3}$	(D=1) * Antibody Levels	-0.1016	0.9536	[-1.9728, 1.7355]	0.4633
$\beta_{D2,1}$	(D=2)	1.7409	0.2527	[1.2549, 2.2433]	1
$\beta_{D2,2}$	(D=2) * Pathogen Load	0.0469	0.9886	[-1.8529, 1.9786]	0.5105
$\beta_{D2,3}$	(D=2) * Antibody Levels	0.3826	0.9035	[-1.4137, 2.1628]	0.6617
$\beta_{D3,1}$	(D=3)	-0.7736	0.6895	[-2.1861, 0.5285]	0.1263
$\beta_{D3,2}$	(D=3) * Pathogen Load	-0.0041	0.9991	[-1.9845, 1.9494]	0.4983
$\beta_{D3,3}$	(D=3) * Antibody Levels	0.1259	0.9875	[-1.8258, 2.0582]	0.5521
$\alpha_{D,1}$	Intercept	0.6887	0.9354	[-1.1200, 2.5174]	0.7679
$\alpha_{D,2}$	Age group	0.9730	0.8063	[-0.5359, 2.6314]	0.8853
$\alpha_{D,3}$	SNAP results	0.9014	0.8253	[-0.6646, 2.5676]	0.8610
$\alpha_{D,4}$	DPP results	0.0473	0.9994	[-1.8891, 2.0141]	0.5183
$\alpha_{D,5}$	Treatment group	0.9217	0.8372	[-0.6550, 2.6156]	0.8682

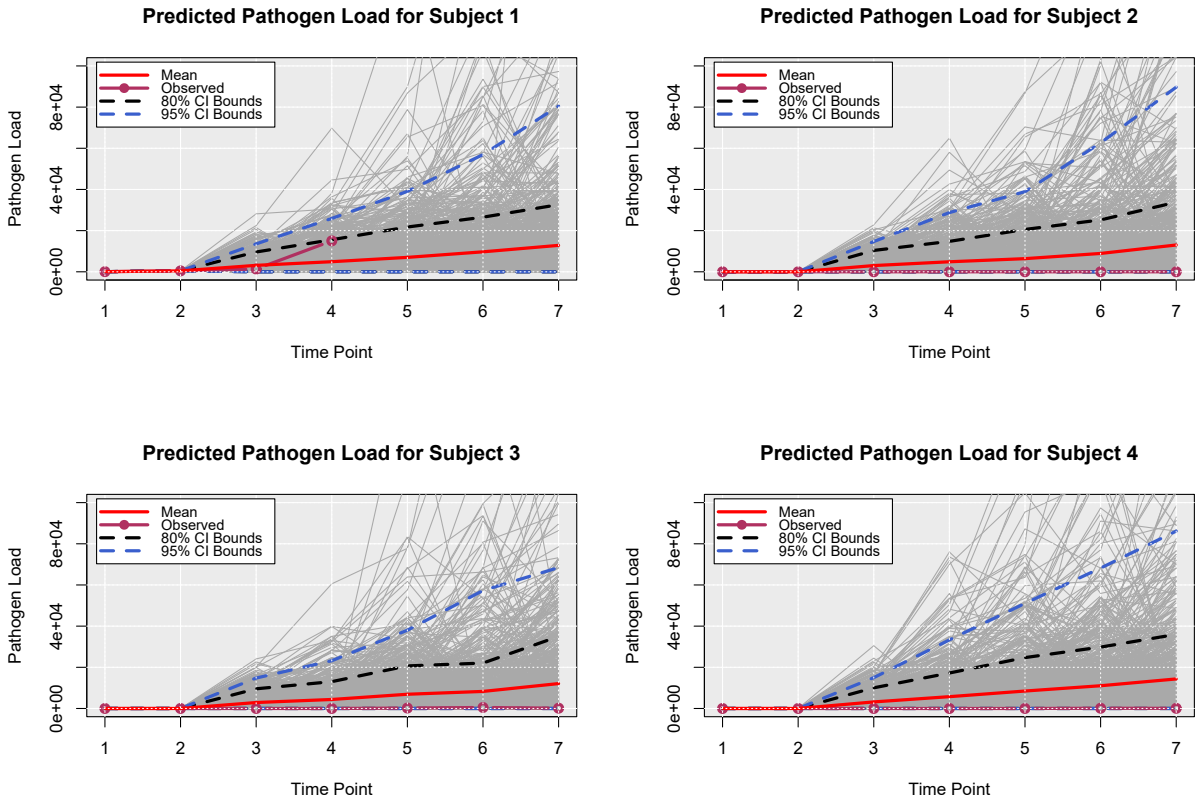

FIGURE 3 Posterior Predictive Trajectories of Pathogen Load. Posterior predicted pathogen load for four dogs. Time points 3 through 7 were predicted times.

where practical due to their ability to formally quantify uncertainty concerning model parameters, rather than relying on simple optimization to provide a "best fit". From the same Figure 1, we saw that at each time point, the observed and latent measures which characterize the pathogen-host dynamics and their interactions comprise the state of the model. Using a hierarchical structure under distributional assumptions is one way to model the evolution of a disease[28,22], allowing us to draw conclusions and quantify uncertainty about important variables related to immune response to infections. In addition, a hierarchical model under the Bayesian setting also enables us to easily handle unobserved values as latent quantities and to estimate them from the available data and model structure[21].

Through this statistical analysis, we were able to explore and characterize some evidence for the processes that drive CanL progression and the host immune response to infection. We investigated the degree to which the presented Bayesian model can predict individual and aggregate patterns of disease progression. We noticed that even when the observed data was collected in 3 month intervals, making predictions in this time frame is not recommended since the disease progression pattern may not yet be apparent. As it was shown with the forecasting scenarios, the presented model specification is still considered to be too simple to fully understand the disease progression and immune responses, and further considerations need to be undertaken to model this complex disease. For instance, considering CD4+ T proliferation over time, and information on different important cytokine expression such as protective inferferon-gamma (IFN-gamma) or inhibitory interleukin 10 (IL-10) could improve the model and its predictions[3]. Although the induction of CD4+ T helper 1 cell responses is considered essential for immunity against *Leishmania*, B cells and the production of *Leishmania*-specific antibodies have also been proposed to play an important role in disease progression[13].

Therefore, an extended version of this model will consider additional important immunological parameters controlling CanL disease presentation, such *Leishmania*-antigen specific CD4+ T cell proliferation, IL-10, and IFN-gamma production. Based on Nylén and Gautam[30], high levels of *Leishmania* specific antibodies are observed in subjects with VL and other severe forms

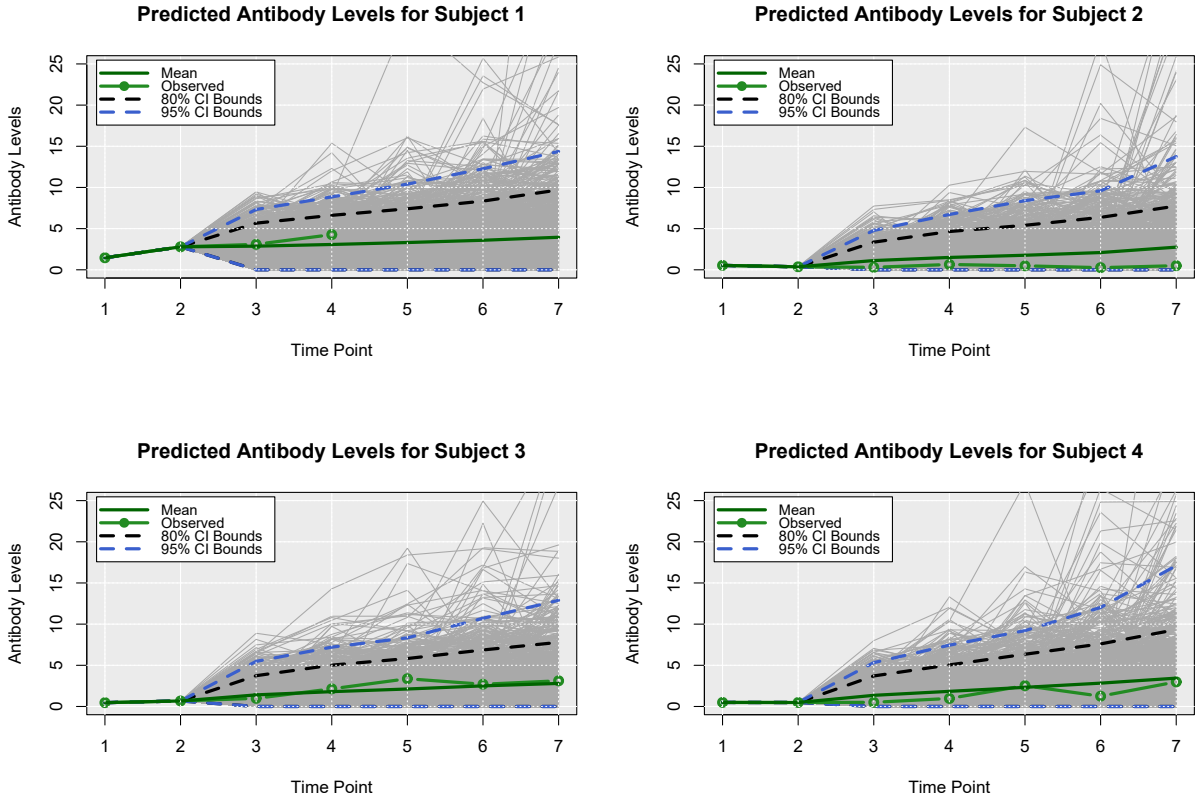

FIGURE 4 Posterior Predictive Trajectories of Antibody Levels. Posterior predicted antibodies level for four dogs. Time points 3 through 7 were predicted times.

of Leishmanial disease and there are accumulating evidence that B cells and antibodies correlate with pathology. Future work incorporating these enhancements, and additional post-study longitudinal follow-up of the canine cohort should enable us to better understand CanL progression, and to refine the predictive performance of the models to create a useful clinical tool.

6 | ACKNOWLEDGEMENTS

Research reported in this article was supported by the National Institutes of Allergy and Infectious Diseases (NIAID) of the National Institutes of Health (NIH) of the United States of America under award number R01AI139267-03 and by MFHA18441000. This work was also performed while B.M.S. was supported by NIH/NIAID T32AI007260, which was the basis for data collection. The content is solely the responsibility of the authors and does not necessarily represent the official views of the National Institutes of Health.

7 | CONFLICT OF INTEREST

The authors declare that there is no conflict of interest.

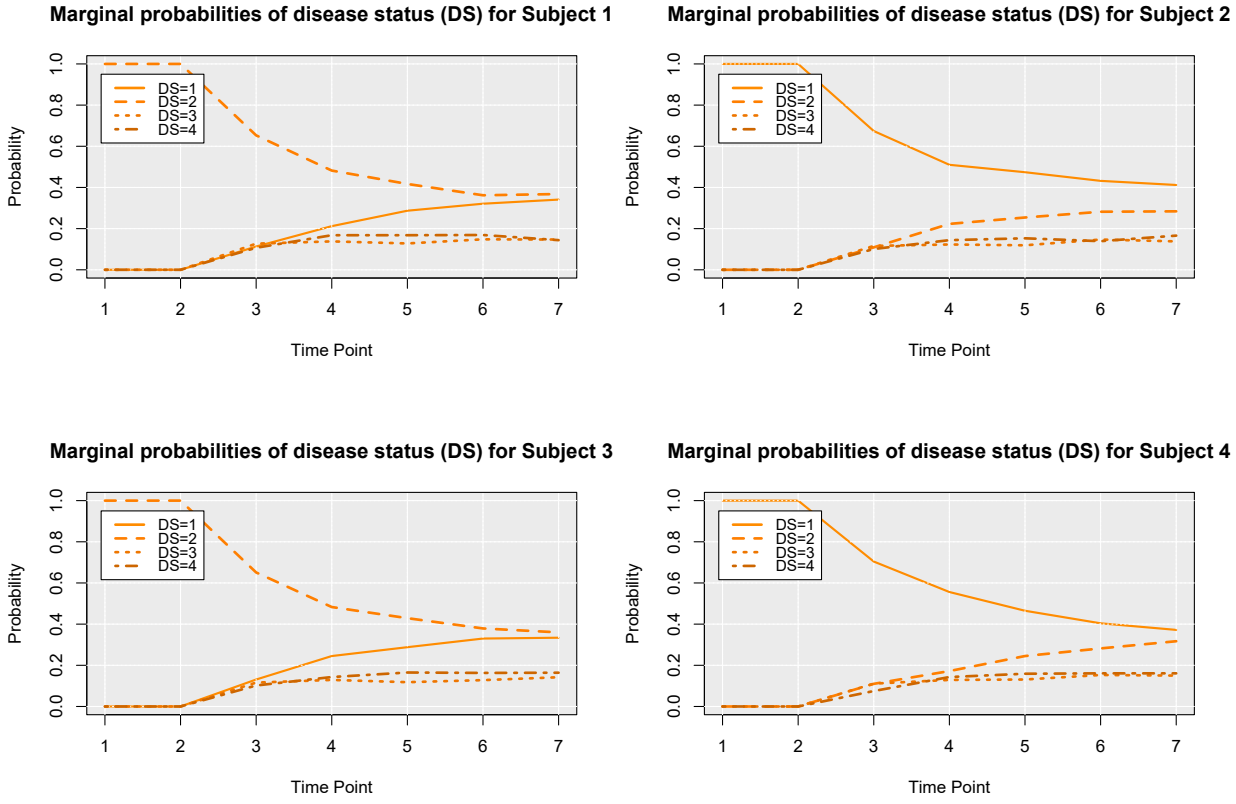

FIGURE 5 Posterior Marginal Probabilities of Disease Status. Posterior predicted (marginal) probabilities of four dogs of being in a particular disease state over time. Time points 3 through 7 were predicted times. Time point 1 corresponds to observed disease state and MCMC estimated latent values were used for time point 2.

8 | DATA AVAILABILITY STATEMENT

The authors confirm that the data analyzed supporting the findings of this study are available within the article and supplementary materials.

9 | ORCID

Felix M. Pabon-Rodriguez https://orcid.org/0000-0003-3528-2354
Grant D. Brown https://orcid.org/0000-0002-7247-7313
Breanna M. Scorza https://orcid.org/0000-0002-3489-0270
Christine A. Petersen https://orcid.org/0000-0002-7285-4254

References

1. Burza S, Croft S, Boelaert M. Leishmaniasis. *The Lancet* 2018; 392(10151): 951–970.

2. Lima ÁL, Lima dID, Coutinho JF, et al. Changing epidemiology of visceral leishmaniasis in northeastern Brazil: a 25-year follow-up of an urban outbreak. *Transactions of the Royal Society of Tropical Medicine and Hygiene* 2017; 111(10): 440–447.

3. Esch KJ, Juelsgaard R, Martinez PA, Jones DE, Petersen CA. Programmed Death 1–mediated T cell exhaustion during visceral leishmaniasis impairs phagocyte function. *The Journal of Immunology* 2013; 191(11): 5542–5550.

4. Barbiéri CL. Immunology of canine leishmaniasis. *Parasite immunology* 2006; 28(7): 329–337.

5. Borja LS, Sousa dOMF, Silva Solcà dM, et al. Parasite load in the blood and skin of dogs naturally infected by Leishmania infantum is correlated with their capacity to infect sand fly vectors. *Veterinary Parasitology* 2016; 229: 110–117.

6. Boggiatto PM, Ramer-Tait AE, Metz K, et al. Immunologic Indicators of Clinical Progression during Canine L eishmania infantum Infection. *Clinical and Vaccine Immunology* 2010; 17(2): 267–273.

7. Solano-Gallego L, Miró G, Koutinas A, et al. LeishVet guidelines for the practical management of canine leishmaniosis. *Parasites & vectors* 2011; 4(1): 1–16.

8. Baxarias M, Álvarez-Fernández A, Martínez-Orellana P, et al. Does co-infection with vector-borne pathogens play a role in clinical canine leishmaniosis?. *Parasites & vectors* 2018; 11(1): 1–16.

9. Mabbott NA. The influence of parasite infections on host immunity to co-infection with other pathogens. *Frontiers in immunology* 2018; 9: 2579.

10. Toepp AJ, Monteiro GR, Coutinho JF, et al. Comorbid infections induce progression of visceral leishmaniasis. *Parasites & vectors* 2019; 12(1): 1–12.

11. Schaut RG, Grinnage-Pulley TL, Esch KJ, et al. Recovery of antigen-specific T cell responses from dogs infected with Leishmania (L.) infantum by use of vaccine associated TLR-agonist adjuvant. *Vaccine* 2016; 34(44): 5225–5234.

12. Figueiredo FB, Vasconcelos TCBd, Madeira MdF, et al. Validation of the Dual-path Platform chromatographic immunoassay (DPP® CVL rapid test) for the serodiagnosis of canine visceral leishmaniasis. *Memórias do Instituto Oswaldo Cruz* 2018; 113.

13. Rossi M, Fasel N. How to master the host immune system? Leishmania parasites have the solutions!. *International immunology* 2018; 30(3): 103–111.

14. Nylén S, Kumar R. Immunobiology of visceral leishmaniasis. *Frontiers in immunology* 2012; 3: 251.

15. Shang Lm, Peng Wp, Jin Ht, et al. The prevalence of canine Leishmania infantum infection in Sichuan Province, southwestern China detected by real time PCR. *Parasites & vectors* 2011; 4(1): 1–5.

16. Rao Kadiyala K, Karlsson S. Forecasting with generalized bayesian vector auto regressions. *Journal of Forecasting* 1993; 12(3-4): 365-378.

17. LeSage JP, Krivelyova A. A Spatial Prior for Bayesian Vector Autoregressive Models. *Journal of Regional Science* 1999; 39(2): 297-317.

18. Holden K. A comparison of forecasts from UK economic models and some Bayesian vector autoregressive models. *Journal of Economic Studies* 1997.

19. R Core Team . *R: A Language and Environment for Statistical Computing*. R Foundation for Statistical Computing; Vienna, Austria: 2022.

20. RStudio Team . *RStudio: Integrated Development Environment for R*. RStudio, PBC; Boston, MA: 2022.

21. Liu JS, Liu JS. *Monte Carlo strategies in scientific computing*. 10. Springer . 2001.

22. Carlin BP, Louis TA. *Bayesian methods for data analysis*. CRC Press . 2008.

23. Plummer M, Best N, Cowles K, Vines K. CODA: convergence diagnosis and output analysis for MCMC. *R news* 2006; 6(1): 7–11.

24. Corthay A. How do regulatory T cells work?. *Scandinavian journal of immunology* 2009; 70(4): 326–336.

25. Mauri C, Bosma A. Immune regulatory function of B cells. *Annual review of immunology* 2012; 30: 221–241.

26. Sompayrac LM. *How the immune system works*. John Wiley & Sons . 2019.

27. Petersen CA. Leishmaniasis, an emerging disease found in companion animals in the United States. *Topics in companion animal medicine* 2009; 24(4): 182–188.

28. Gelman A, Carlin JB, Stern HS, Rubin DB. *Bayesian data analysis*. Chapman and Hall/CRC . 1995.

29. De Finetti B. *Theory of probability: A critical introductory treatment*. 6. John Wiley & Sons . 2017.

30. Nylen S, Gautam S. Immunological perspectives of leishmaniasis. *Journal of global infectious diseases* 2010; 2(2): 135.

31. Cragg JG. Some Statistical Models for Limited Dependent Variables with Application to the Demand for Durable Goods. *Econometrica* 1971; 39(5): 829–844.

How to cite this article: Pabon-Rodriguez, F., Brown, G., Scorza, B., and Petersen, C. (2022), Bayesian Hierarchical Model for Immune Responses to Leishmania-tick borne Co-Infection Study, *Statistics in Medicine*, *2022;??:?–?*.

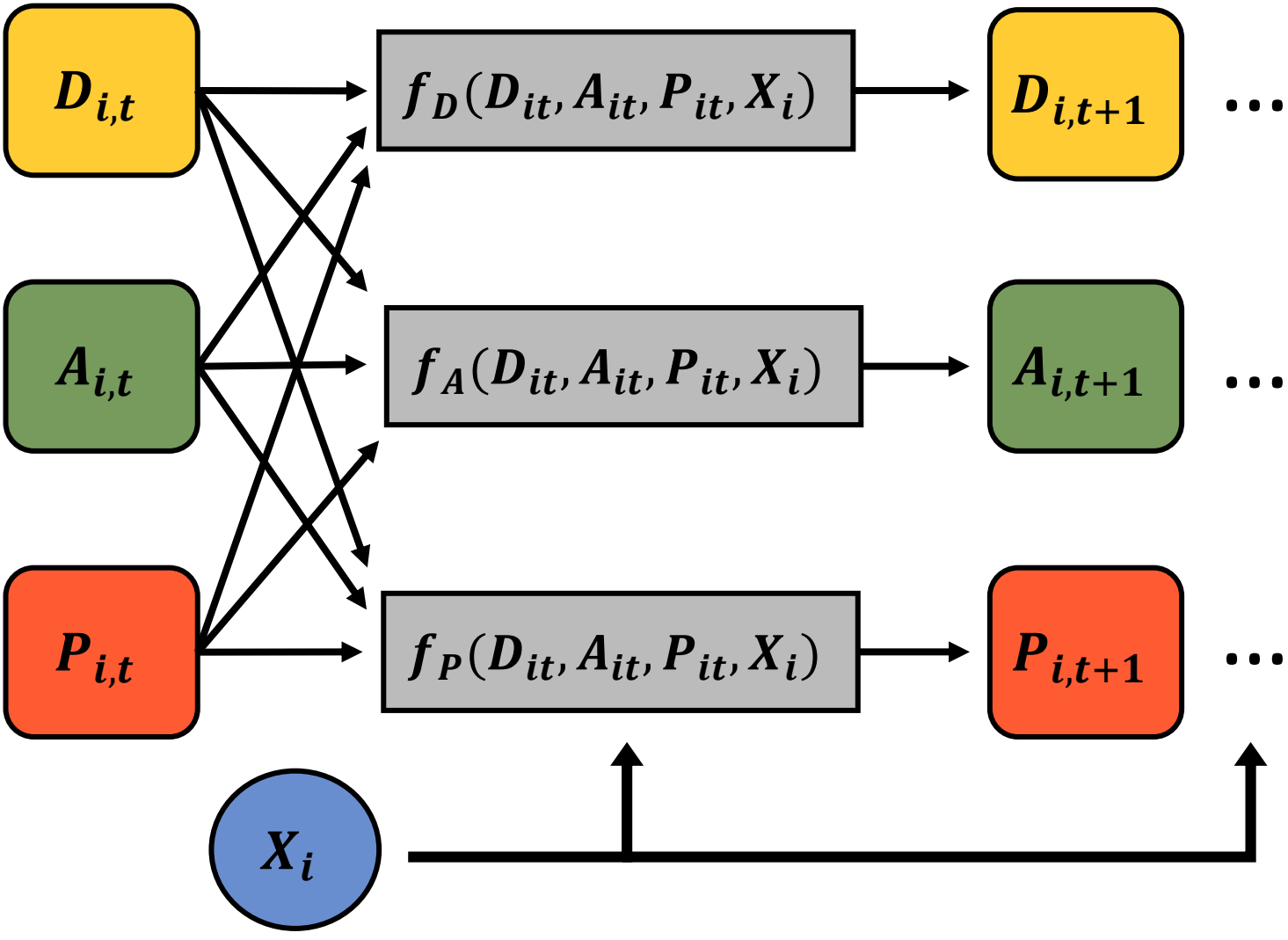
$D_{i,t}$
$A_{i,t}$
$P_{i,t}$
X_i
$f_D(D_{it}, A_{it}, P_{it}, X_i)$
$f_A(D_{it}, A_{it}, P_{it}, X_i)$
$f_P(D_{it}, A_{it}, P_{it}, X_i)$
$D_{i,t+1}$
$A_{i,t+1}$
$P_{i,t+1}$
...
...
...

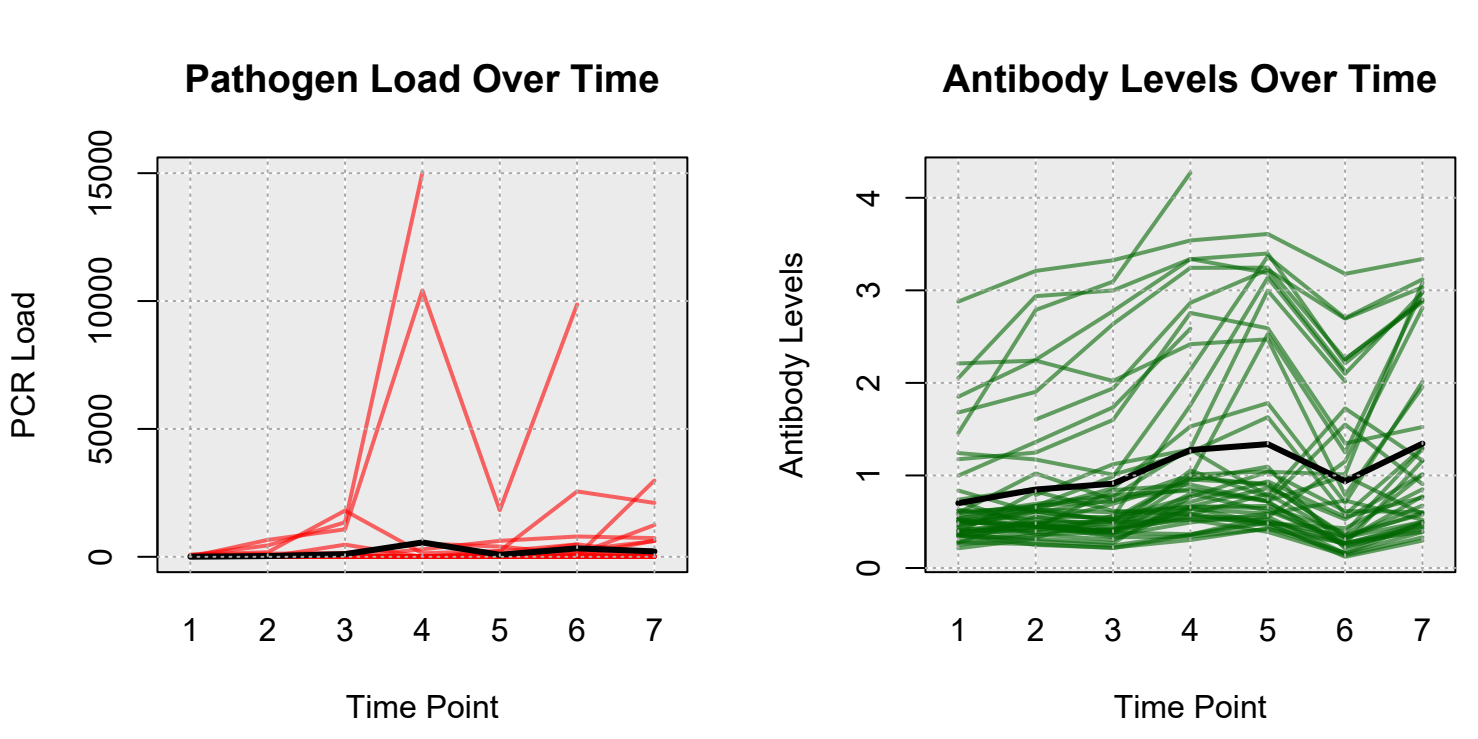
Pathogen Load Over Time
PCR Load
0
5000
10000
15000
1
2
3
4
5
6
7
Time Point
Antibody Levels Over Time
Antibody Levels
0
1
2
3
4
1
2
3
4
5
6
7
Time Point

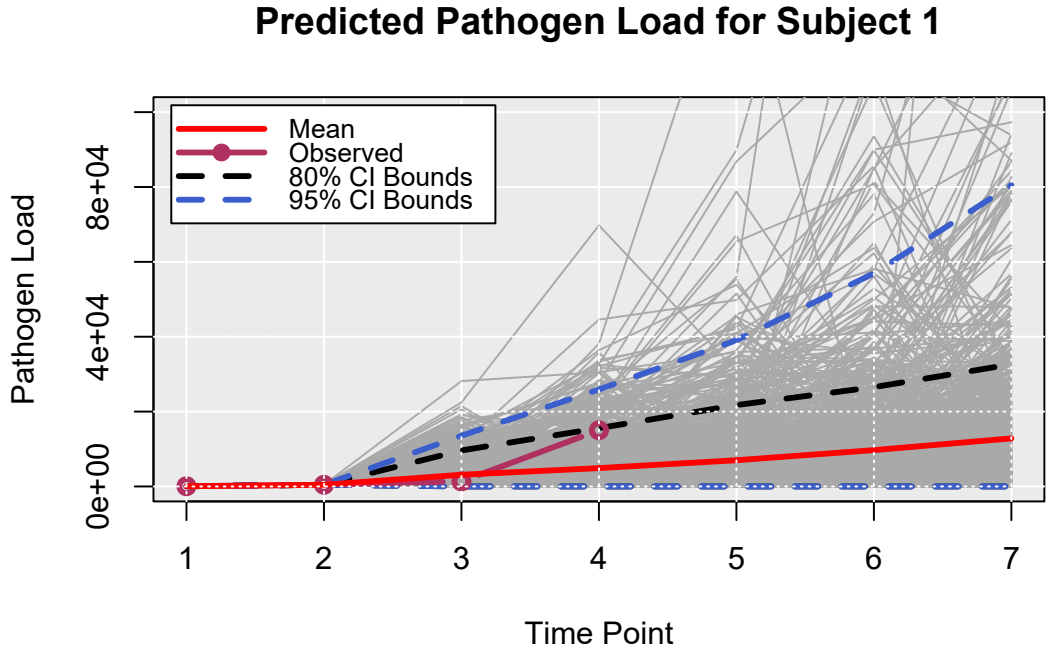
Predicted Pathogen Load for Subject 1
Mean
Observed
80% CI Bounds
95% CI Bounds
Pathogen Load
0e+00
4e+04
8e+04
1
2
3
4
5
6
7
Time Point

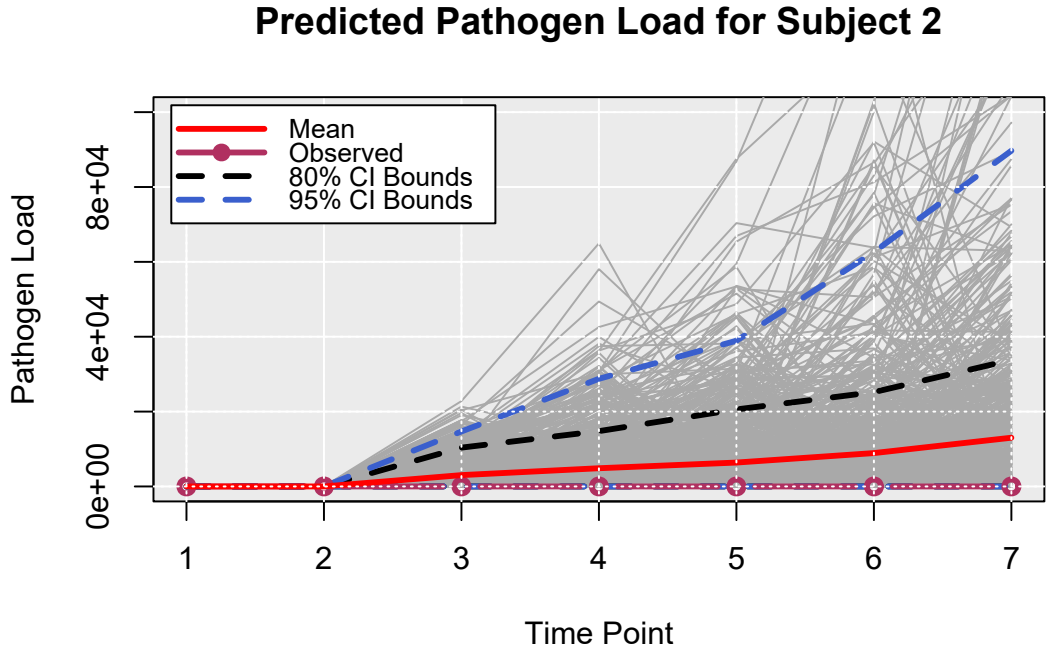
Predicted Pathogen Load for Subject 2
Mean
Observed
80% CI Bounds
95% CI Bounds
Pathogen Load
0e+00
4e+04
8e+04
1
2
3
4
5
6
7
Time Point

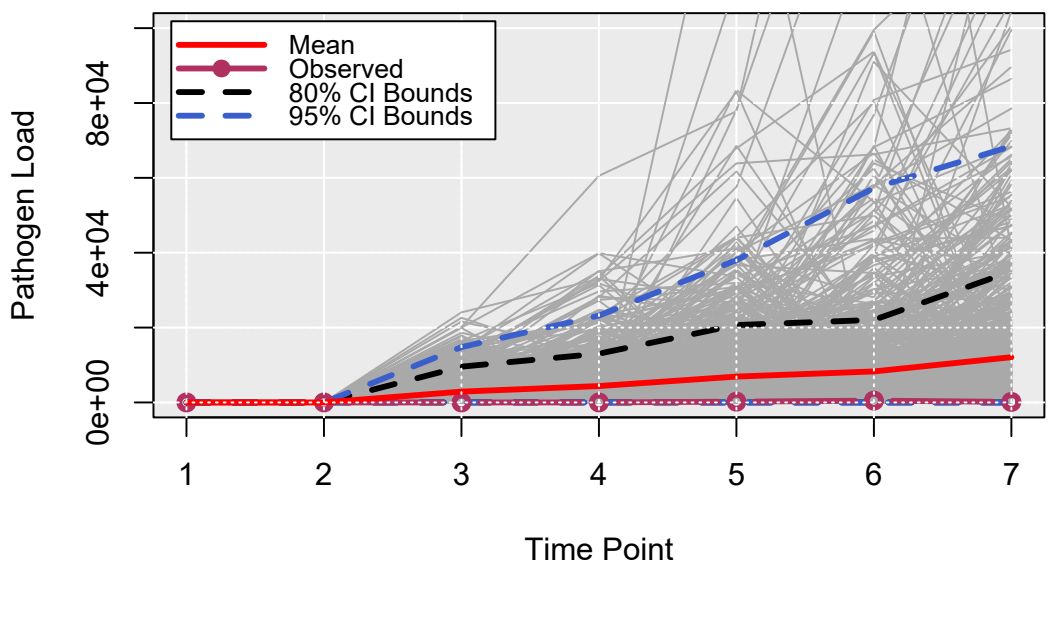
Predicted Pathogen Load for Subject 3
Mean
Observed
80% CI Bounds
95% CI Bounds
Pathogen Load
0e+00
4e+04
8e+04
1
2
3
4
5
6
7
Time Point

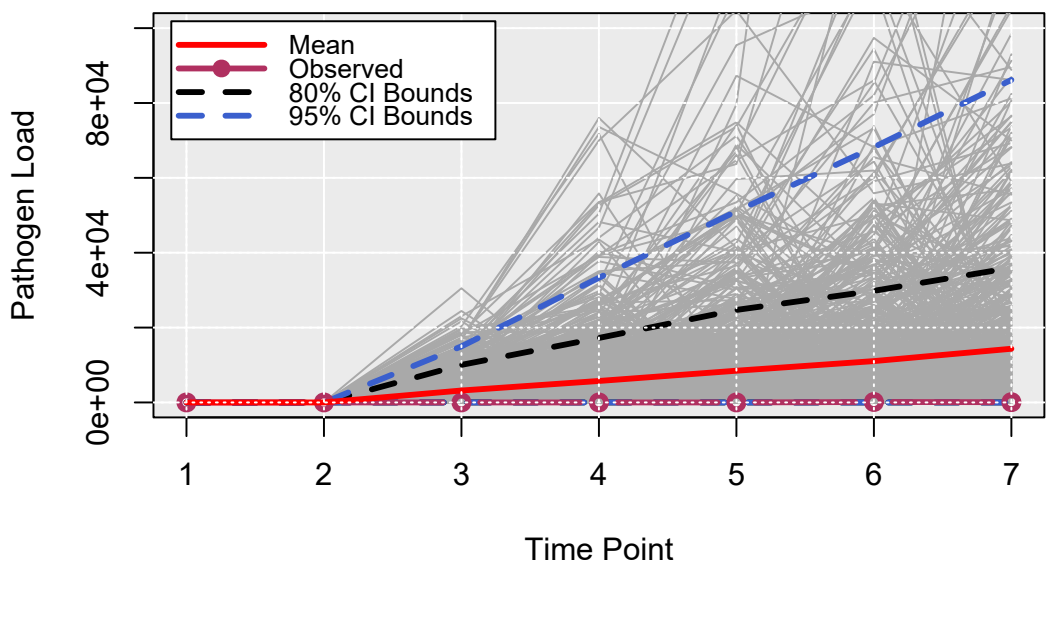
Predicted Pathogen Load for Subject 4
Mean
Observed
80% CI Bounds
95% CI Bounds
Pathogen Load
0e+00
4e+04
8e+04
1
2
3
4
5
6
7
Time Point

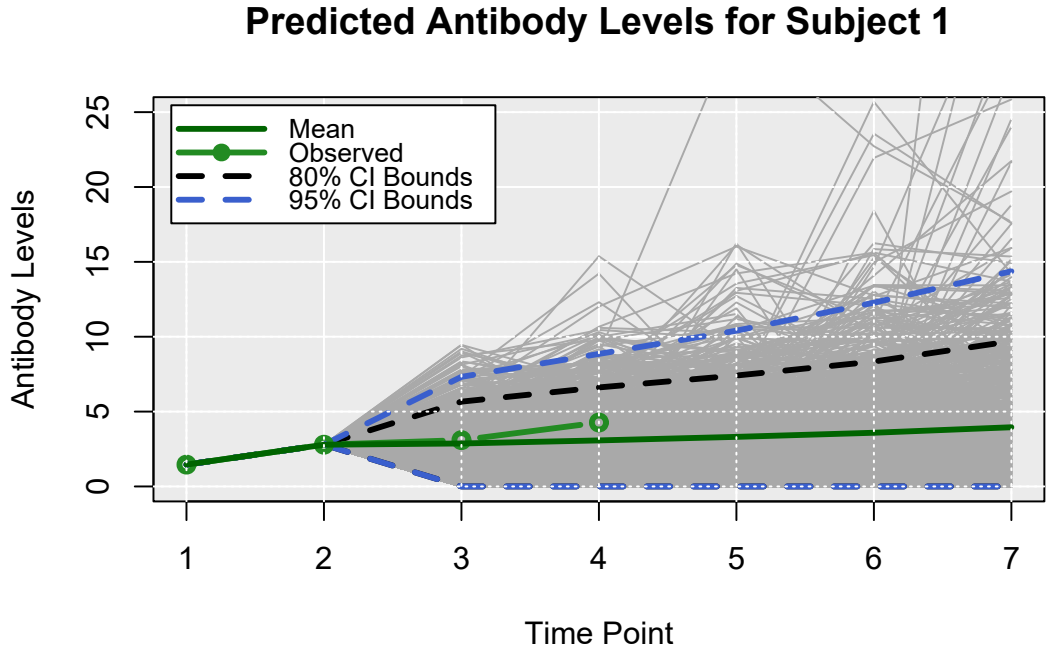
Predicted Antibody Levels for Subject 1
Mean
Observed
80% CI Bounds
95% CI Bounds
Antibody Levels
0
5
10
15
20
25
1
2
3
4
5
6
7
Time Point

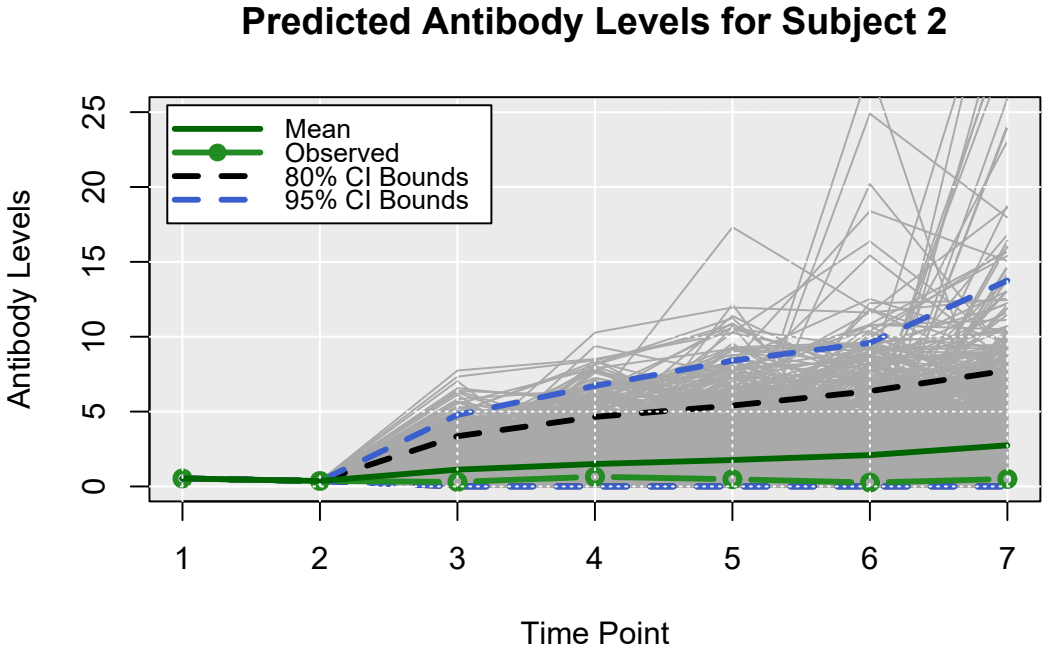
Predicted Antibody Levels for Subject 2
Mean
Observed
80% CI Bounds
95% CI Bounds
Antibody Levels
0
5
10
15
20
25
1
2
3
4
5
6
7
Time Point

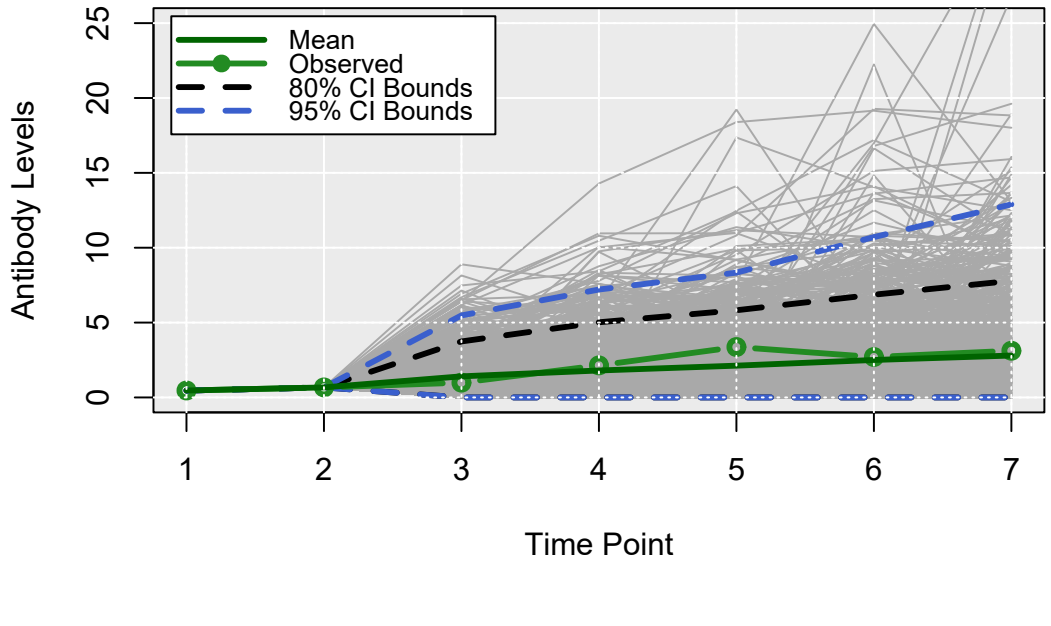
Predicted Antibody Levels for Subject 3
Mean
Observed
80% CI Bounds
95% CI Bounds
Antibody Levels
0
5
10
15
20
25
1
2
3
4
5
6
7
Time Point

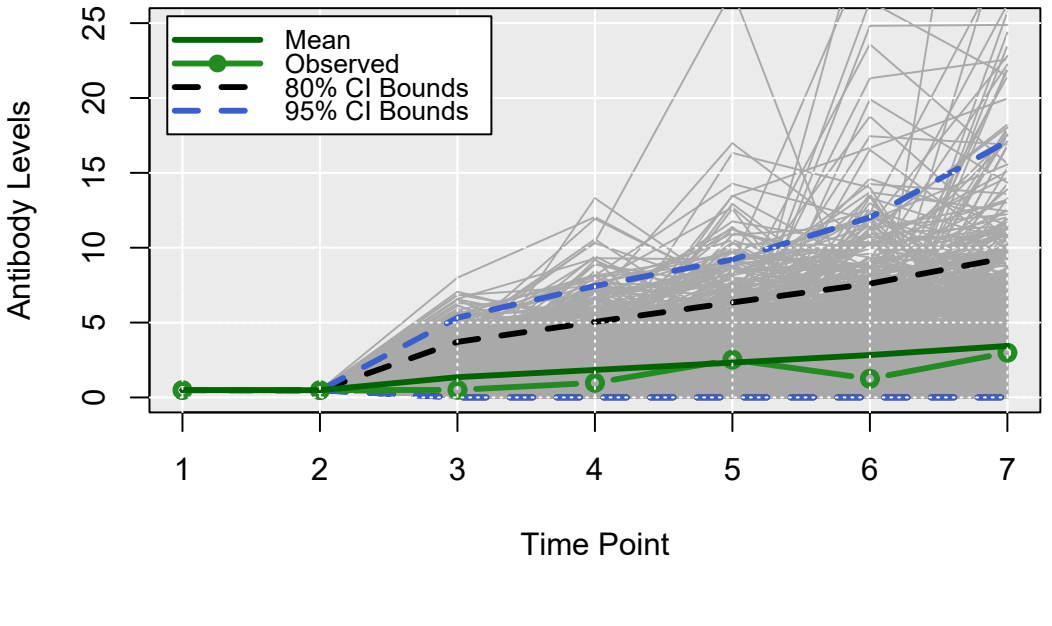
Predicted Antibody Levels for Subject 4
Mean
Observed
80% CI Bounds
95% CI Bounds
Antibody Levels
0
5
10
15
20
25
1
2
3
4
5
6
7
Time Point

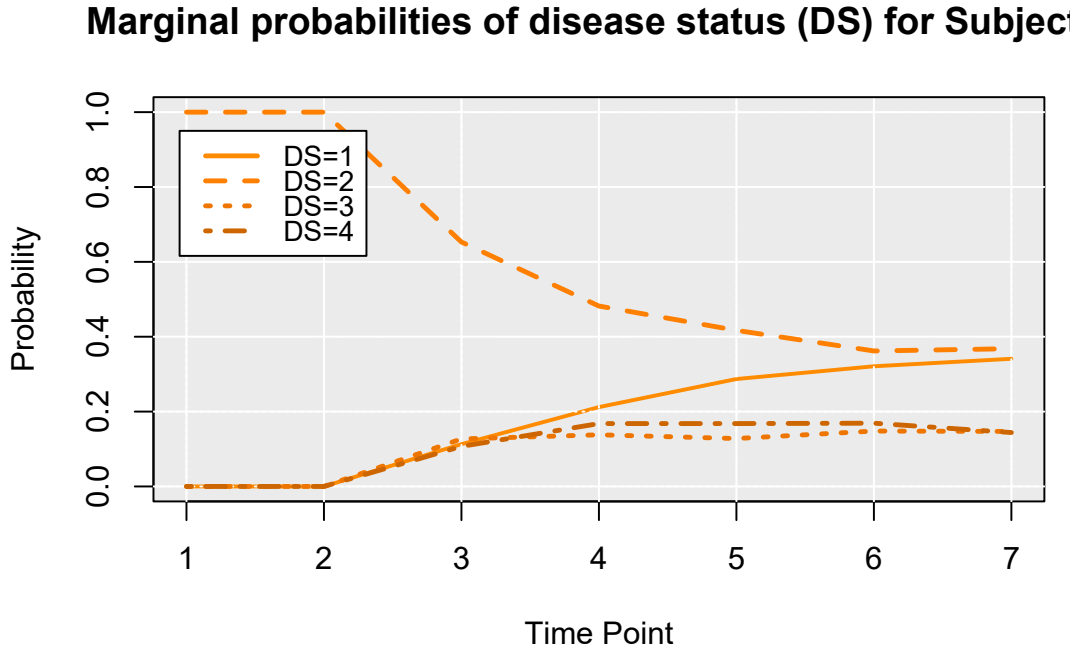
Marginal probabilities of disease status (DS) for Subject 1
Probability
0.0
0.2
0.4
0.6
0.8
1.0
DS=1
DS=2
DS=3
DS=4
1
2
3
4
5
6
7
Time Point

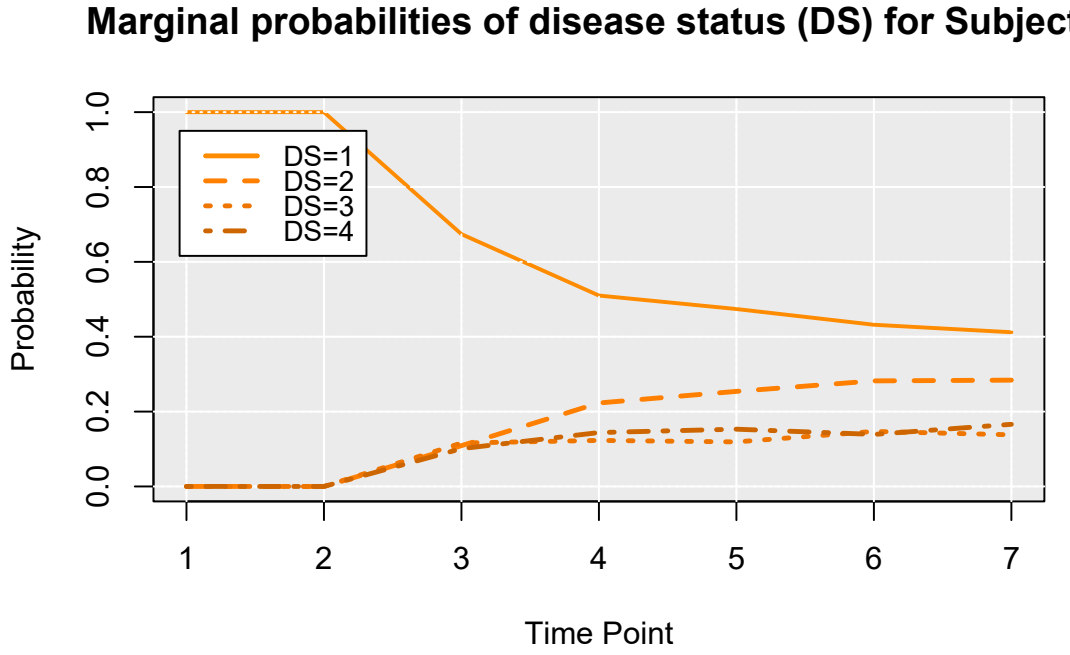
Marginal probabilities of disease status (DS) for Subject 2
Probability
0.0
0.2
0.4
0.6
0.8
1.0
DS=1
DS=2
DS=3
DS=4
1
2
3
4
5
6
7
Time Point

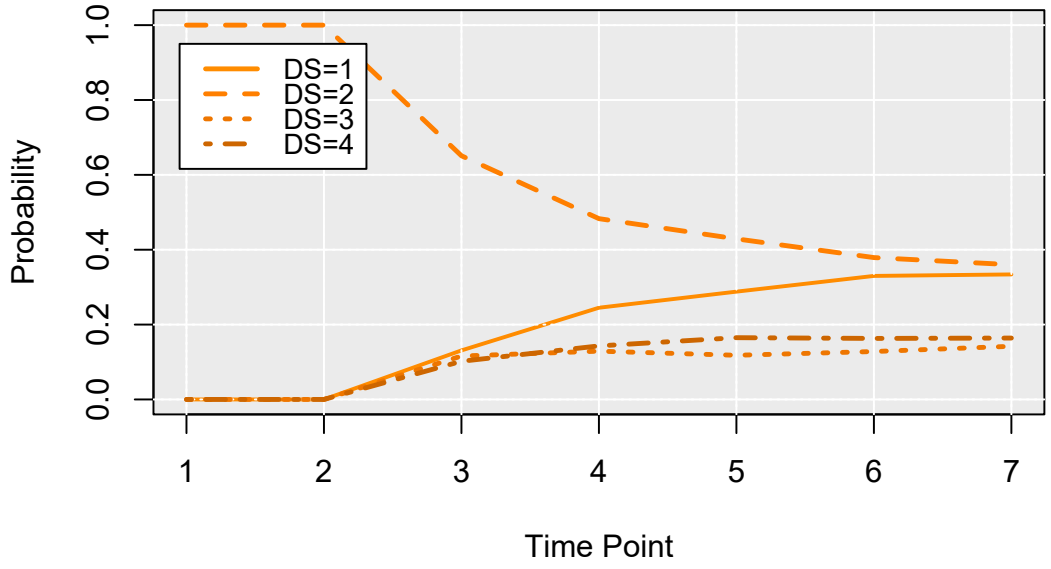
Marginal probabilities of disease status (DS) for Subject 3
Probability
0.0
0.2
0.4
0.6
0.8
1.0
DS=1
DS=2
DS=3
DS=4
1
2
3
4
5
6
7
Time Point

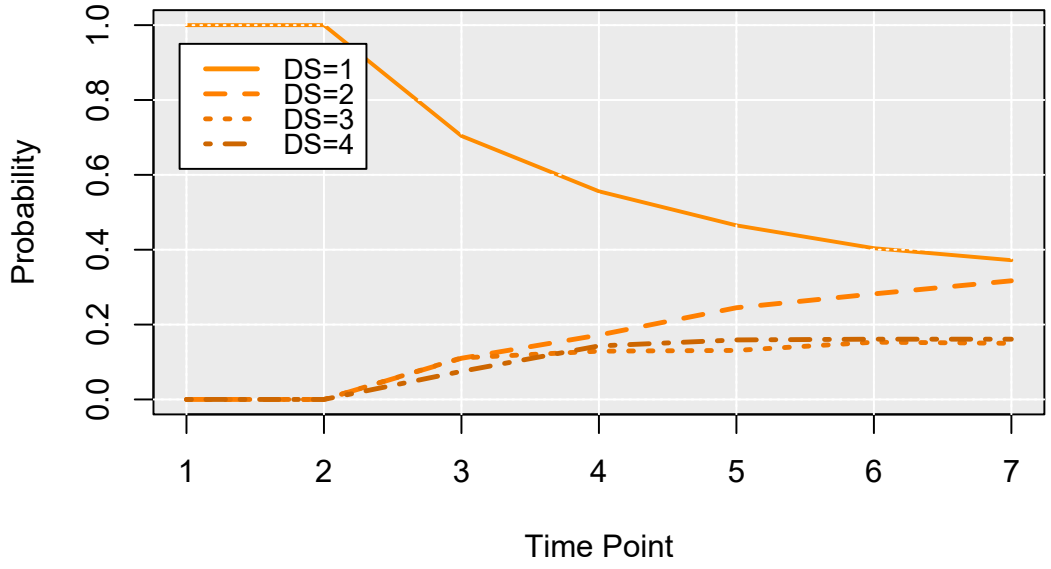
Marginal probabilities of disease status (DS) for Subject 4
Probability
0.0
0.2
0.4
0.6
0.8
1.0
DS=1
DS=2
DS=3
DS=4
1
2
3
4
5
6
7
Time Point